ANALYSIS OF HYPEROSMOTIC CHANGES IN TIGHT JUNCTIONS
USING IMMUNOCYTOCHEMISTRY AND ELECTRIC
CELL-SUBSTRATE IMPEDENCE SENSING

AN ABSTRACT

SUBMITTED ON THE FIFTH DAY OF MAY 2021

TO THE DEPARTMENT OF BIOMEDICAL ENGINEERING

IN PARTIAL FULFILLMENT OF THE REQUIREMENTS

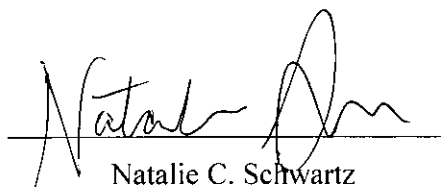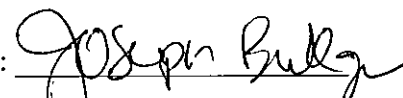OF THE SCHOOL OF SCIENCE AND ENGINEERING

OF TULANE UNIVERSITY

FOR THE DEGREE

OF

MASTER OF SCIENCE IN BIOMEDICAL ENGINEERING

BY

_____
Natalie C. Schwartz

Approved: _____
Joseph L. Bull, Ph.D.

_____
Donald P. Gaver, Ph.D.

_____
Eiichiro Yamaguchi, Ph.D.

## <u>ABSTRACT</u>

The blood-brain barrier (BBB) consists of specialized endothelial cells (EC) tightly interconnected by transmembrane proteins that form tight junctions (TJ). This separates the central nervous system (CNS) from systemic blood and protects the brain from harmful circulating substances. The essential defensive properties that permit such tight transport regulation also prevent most drugs from reaching the CNS. A standard method of CNS drug delivery has yet to be established in clinical settings. Mannitol is a hyperosmotic agent that has the ability to transiently open the BBB without causing permanent damage. Mannitol exposure causes hyperosmotic shock, which draws water out of endothelial cells and causes them to shrink, producing a temporary opening between TJs. Electrical Cell-Substrate Impedance Sensing (ECIS) measures the complex impedance of cell monolayers across the frequency spectrum in order to differentiate between junctional resistance, or the "tightness" of cell-to-cell contact, normal impedance, which is caused by cell-substrate interaction, and cell membrane capacitance. The purpose of this thesis is to elucidate the mechanisms that cause hyperosmotic TJ opening and evaluate the potential application of mannitol for BBB opening. Real-time electrical data was collected before and after the introduction of varying concentrations and durations of mannitol treatment. Imaging analysis and resistance data revealed valuable insights into TJ opening behavior and barrier recovery mechanisms. Hyperosmotic shock has a significant effect on monolayer permeability, but further research is warranted in order to understand how the changes in cellular behavior can be applied to the development of safe therapeutic applications.

ANALYSIS OF HYPEROSMOTIC CHANGES IN TIGHT JUNCTIONS
USING IMMUNOCYTOCHEMISTRY AND ELECTRIC
CELL-SUBSTRATE IMPEDENCE SENSING

A THESIS

SUBMITTED ON THE FIFTH DAY OF MAY 2021

TO THE DEPARTMENT OF BIOMEDICAL ENGINEERING

IN PARTIAL FULFILLMENT OF THE REQUIREMENTS
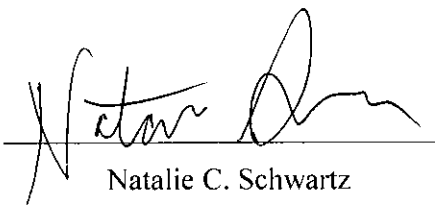
OF THE SCHOOL OF SCIENCE AND ENGINEERING

OF TULANE UNIVERSITY

FOR THE DEGREE

OF

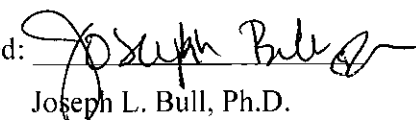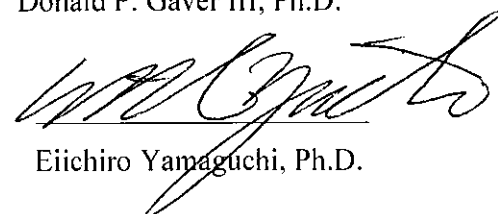MASTER OF SCIENCE IN BIOMEDICAL ENGINEERING

BY

_____
Natalie C. Schwartz


Approved: _____
Joseph L. Bull, Ph.D.

_____
Donald P. Gaver III, Ph.D.

_____
Eiichiro Yamaguchi, Ph.D.

# **<u>ACKNOWLEDGEMENTS</u>**

# Table of Contents

# LIST OF FIGURES

# 1. <u>INTRODUCTION</u>

The human body's central nervous system is separated from general circulation by a specialized endothelium called the blood-brain barrier (BBB). This endothelial monolayer is a phenomenon of interconnected systems working together to maintain overall homeostasis and ensure healthy physiological functions. The structural and physiological characteristics of the BBB are generally related to the unique tight junctions (TJ) that seal adjacent endothelial cells (EC) together. These junctions make it extremely difficult for hydrophilic or polar drug molecules to pass through the BBB and reach the CNS. In fact, this tightly regulated, and highly selective transport system prevents an estimated 98% of small molecules and 100% of large molecules from entering the CNS in therapeutic quantities (1). Although an essential component of physiological homeostasis, this biological membrane has continued to pose a major challenge for successful treatment of CNS diseases. Drug development time for CNS drugs tends to be significantly longer than for non-CNS drugs (2). There are potential therapies out there for various CNS diseases, but the issue of efficacious drug delivery continues to stand in the way. A clinical standard to open the BBB must be established or CNS diseases will continue to affect millions of people and remain the leading cause of disability in the world (3).

There are many different avenues being explored to safely open the BBB and deliver therapeutic quantities of drugs to the CNS. Osmotic diuretics such as mannitol show potential for the transient opening of the BBB, but in clinical settings have resulted

in side effects on the brain (2). The presence of a hyperosmotic agent causes ECs to shrink, which results in the stretching of transmembrane proteins and the opening of small holes within TJs. Mannitol is a pharmacologically inert substance that inhibits reabsorption of water and sodium. It is commonly given intravenously for hyperosmolar treatment of cerebral edema because it expands extracellular fluid and plasma volume outside the BBB, which locally reduces the plasma volume in the nervous system. The movement of fluids from the brain parenchyma to the intravascular space lowers intracranial pressure and effectively resolves most cases of cerebral edema. However, there are high rates of adverse effects that include hypotension, seizure, and brain swelling (4). Higher concentrations of mannitol have been shown to be more effective for BBB opening but are supplemented by a higher risk of adverse events (5). The overall effect of mannitol dosing, concentration, and length of action need to be further understood in order to establish a safe and effective procedure of BBB opening.

Mannitol's effects on TJs can be measured using electrical and visual data. Impedance measurements are extremely useful in the characterization of barrier integrity because of the distinguishment between paracellular junctional changes or changes in basal adhesion based on a collection of real-time measurements at various frequencies. Fluorescent images support the interpretations of impedance changes and can provide further information on the changes of specific cellular components. The primary goal of this project was to determine if ECIS and immunocytochemistry can effectively analyze hyperosmotic TJ changes.

## 2. BACKGROUND

*2.1 The Blood-Brain Barrier*

The BBB is a highly selective boundary that prevents solutes circulating in the bloodstream from crossing into the extracellular fluid of the nervous system. It blocks the entry of materials such as toxins, pathogens, and other large molecules by maintaining unique TJs, adherens junctions (AJ) and a highly selective permeability. The specialized ECs that form the BBB are absent of fenestrations and have a small number of endocytic vesicles compared to capillaries located elsewhere in the human body. Therefore, vesicular transport of macromolecules or endocytosis is restricted in these ECs. Paracellular transport is restricted by the tightly fused ECs that close off intercellular spaces. These cellular properties result in highly polarized ECs that regulate the movement of material between the blood and brain.
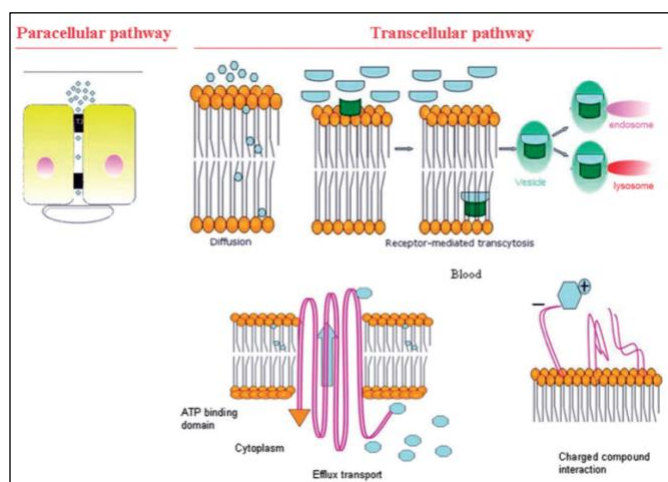


**Figure 1:** The paracellular and transcellular pathways of the blood-brain barrier (6).

The transcellular pathways involve energy-dependent processes like receptor-mediated transcytosis and active efflux processes as well as energy-independent transcellular diffusion (Figure 1). The brain's vessel wall contains selective transporter proteins that facilitate active transport of metabolic products such as glucose and amino acids. Charged compound interaction at the BBB, often referred to as adsorptive-mediated transcytosis (AMT), occurs when positive molecules interact with negatively charged microdomains on the EC membrane (7). The BBB effectively acts as a dynamic interface between the CNS and the rest of the body with the purpose of maintaining brain homeostasis.

2.1.1 The Neurovascular Unit

In order to execute the BBB's specialized functions, vascular cells communicate with other neuronal components such as neurons and glia. The participants of this intercellular signaling make up the multicellular neurovascular unit (NVU). This system of interdependent processes enables the BBB to function as a highly selective barrier for the CNS. The NVU is composed of ECs, neuronal terminations, pericytes, astrocytes, microglia, and the basement membrane. These cellular and extracellular components work together to control hyperemia, aligning local blood supply with neuronal demand, and overall barrier function (8). Pericytes are mural cells embedded in the continuous basement membrane that occupy the space between the ECs and astrocyte end-feet (Figure 2). They play a major role in the development and differentiation of NVU cell types and the regulation of local microvasculature, barrier stability, and angiogenesis.
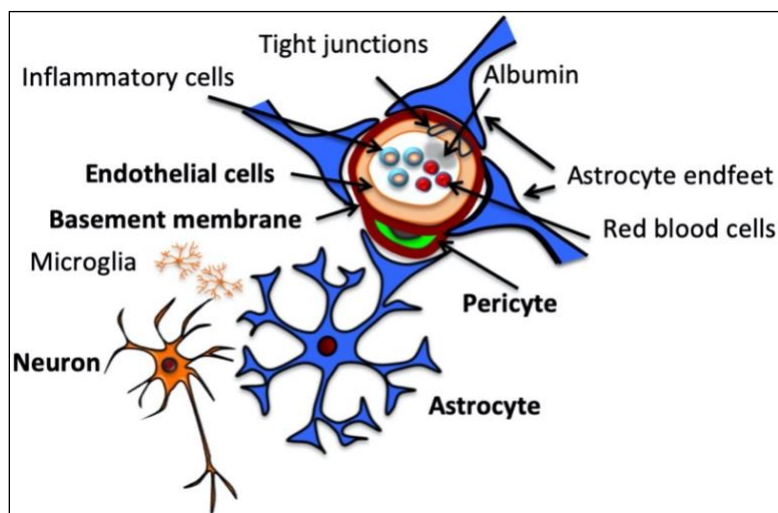
**Figure 2:** The components of the neurovascular unit. The endothelial cells make up the blood-brain barrier (8).

Astrocytes are the most abundant cell type in the nervous system and are positioned between ECs and neurons to modulate neuronal function and maintain microenvironmental equilibrium (9). Astrocyte end-feet cover most of the endothelium, which facilitates bidirectional communication between astrocytes and ECs (8). The basement membrane (BM), also referred to as the basal lamina is made up of a unique extracellular matrix (ECM) that separates ECs from pericytes and astrocyte end feet. The ECM and support proteins of the BM interact with membrane receptors and are essential to proper NVU function (10). The immune responses in the brain are primarily mediated by resident microglia. Perivascular macrophages derived from microglia and circulating bone-marrow monocytes are also present in the NVU and act as the first line of defense against invading pathogens. The overall protection and function of the BBB relies on the integrity of all aforementioned NVU components.

2.1.2 Barrier Transport Mechanisms

Small non-polar molecules, lipid-soluble molecules, and gases such as oxygen are able to passively diffuse through the interior blood vessels of the brain and enter the CNS through paracellular pathways. ECs of the BBB express two main types of transporter proteins: polarized efflux transporters that regulate the diffusive entry of those lipophilic molecules by pushing them out to the blood, and nutrient specific transporters that allow certain materials through the barrier for the purpose of cellular CNS nourishment (11). Efflux transporters are expressed on the blood facing side of the barrier and are driven by ATP hydrolysis to transport endogenous metabolites and other substrates up their concentration gradient into the blood compartment (Figure 3). Nutrient transporters are mainly involved in transporting substrates down their concentration gradient through carrier mediated transport (CMT). This involves the transport of glucose, amino acids, nucleosides, and organic anions and cations from the blood to the brain, which are all essential fuel for different CNS metabolic processes. These transport systems are also important for removal of waste from the CNS.
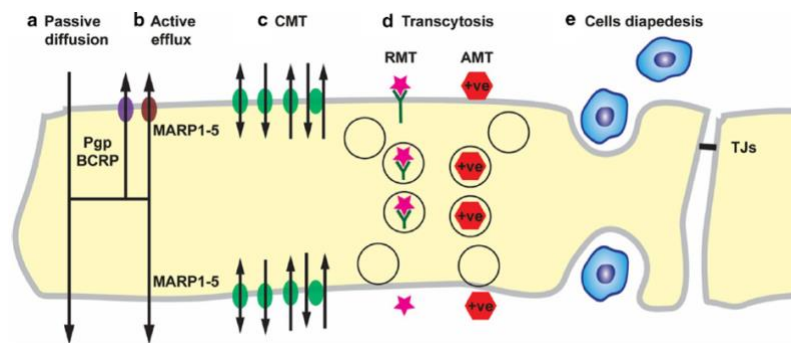


**Figure 3:** The specific barrier transport mechanisms that include **(a)** passive diffusion, **(b)** active efflux, **(c)** carrier-mediated transport, **(d)** Transcytosis (receptor-mediated transport and adsorptive-mediated transport, **(e)** cells diapedesis. (9)

Regulated transport systems maintain important concentration differences between the blood and the brain. For instance, the difference in ion concentration of the blood and brain is relatively small compared to the difference in protein and amino acid concentration of the blood and cerebral spinal fluid. CMT systems cannot facilitate transport of larger peptides and proteins, which means vesicular transport systems such as receptor mediated transport (RMT) and AMT are required in order for large solutes to gain entry to the BBB (9). These transcytotic mechanisms either rely on surface receptors to be internalized and exocytosed or specific cell surface binding sites to pick up large positively charged molecules and bring them into the cell and to the other side of the membrane.

2.1.3 Membrane Proteins

The structural integrity of the BBB relies mainly on transmembrane proteins that fuse together on the outer plasma membrane forming TJs. Three main transmembrane proteins and various cytoplasmic proteins linked to the actin skeleton work together to ensure the unique integrity of the BBB. Occludins are dynamic proteins found exclusively in TJs and play a role in barrier regulation. However, there is evidence that functional TJs can exist in epithelial cells without the presence of occludins. Mice deficient in occludin proteins had CNS calcification, which means occludin most likely plays a role in the regulation of calcium across the BBB (11). This points toward the idea that occludins play a very specific role in BBB TJs by increasing overall membrane electrical resistance and decreasing paracellular permeability of specific solutes (12). Claudins are a family of proteins that are thought to be responsible for the novel seal of BBB junctions by forming dimers and binding homotypically to claudins on adjacent

cells. Junction adhesion molecules (JAMs) are a member of the immunoglobin superfamily and are the third of the crucial transmembrane proteins that work to regulate paracellular permeability. Although more research is required to fully understand their mechanisms, these molecules play a role in cell-cell adhesion and monocyte transmigration (9).
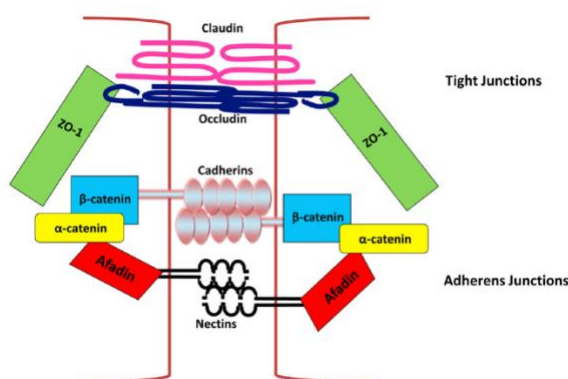


**Figure 4:** The structural relationship between tight and adherens junctions is maintained by the cytoplasmic accessory protein ZO-1 (13).

Cytoplasmic accessory proteins such as zonula occludens proteins ensure the TJs are linked to the cell cytoskeleton. ZO-1 structurally and functionally links TJs to AJs by connecting them via the mutual actin cytoskeleton (Figure 4). AJs attach both cells' microfilaments and exist as a protein layer on the inside of the plasma membrane. They connect all ECs through interactions between extracellular domains of cadherins, which are made up of vascular endothelial (VE)- cadherin and platelet EC adhesion molecules (PECAM). Functionally, VE-cadherin at AJs upregulates gene encoding for the TJ protein claudin-5. These molecules work together to produce the advanced barrier regulation of the BBB, which causes polarization on both sides of the membrane. The highly polarized cells utilize efflux and nutrient transporters expressed in the CNS to control the necessary facilitation of ions and molecules between the blood and the brain.

The diverse transport mechanisms involved in barrier regulation are potential targets for effective drug delivery into the CNS.

*2.2 CNS Drug Delivery*

The defensive properties of the BBB, which is the tightest endothelium in the human body, create a significant obstacle for successful drug delivery into the CNS. Therapeutic drug molecules are often much too large to diffuse through the TJs that connect the endothelial cells of the BBB. Therefore, systemic drug delivery does not result in effective CNS drug concentrations unless administered at dangerously high concentrations. Even so, most drug molecules can be harmful to healthy tissue and require a more targeted delivery approach. Researchers have been searching for a noninvasive method that transiently opens the BBB enough to allow large drug molecules to pass through the BBB and into neural tissue. This requires modification of BBB permeability for a short duration because extended opening can damage the endothelium and cause neuropathological changes, cerebral vasculopathy, and possible seizure (6). Both chemical and physical methods have been tested *in vitro* and *in vivo* but there has still not been a satisfactory, effective procedure established.

2.2.1 BBB Mechanical Disruption

The mechanical disruption of the BBB is mostly due to the disruption of junctional complexes. The application of ultrasound technology has shown massive potential for safe BBB disruption and has proven to non-invasively and transiently increase cell permeability without permanently damaging healthy tissue (14). However, the mechanisms causing the permeability change are poorly understood. Surgical

approaches are commonly used in emergency situations and are extremely invasive.

Direct local drug infusion is a simple drug delivery method but is still not ideal because

of slow diffusion coefficients of many drugs (6).

2.2.2 Targeted Delivery Systems

The majority of non-invasive techniques involve some sort of strategic drug

modification. Large drug molecules are often water-soluble and can be transformed into

lipid-soluble molecules by adding functional groups (15). This enhances the likelihood of

the therapeutic molecules to passively diffuse through the BBB as lipophilicity increases.

Microchip and micro-electromechanical systems technology have been tested as a means

of controlled drug delivery with precise temporal control over release kinetics and target

drug quantities (6). Nanotechnology is another exploding field that has major potential

for drug release in the brain. Nanoparticles have shown to be effective drug carriers and

take advantage of the BBB's innate AMT. However, the challenge of site-specific drug

delivery and efficient drug-loading methods hinder the implementation and

commercialization of nano-delivery systems.

2.2.3 BBB Chemical Disruption

Various methods of chemical disruption have proven to increase the overall

permeability of the BBB. Although these techniques encourage therapeutic drug uptake,

they can also allow harmful substances circulating in the blood to cross over into the

CNS and cause permanent permeability changes. Therefore, the main challenge for

successful chemical disruption is understanding the molecular mechanisms involved,

targeting specific components of the BBB, and ensuring a transient opening that is

followed by recovery. The signaling pathways of vasoactive agents like histamine and

bradykinin have been shown to increase BBB permeability by altering phosphorylation activity at junctional complex proteins and relaxing cell-cell contact (6).

Hyperosmotic shock shows potential as a transient method of opening the BBB and is commonly used in clinical practice for resolving cases of cerebral edema, intra-ocular pressure, and low urine output (16). The presence of hyperosmotic agents such as hypertonic saline or mannitol causes extracellular fluid and plasma to expand by pulling fluid out from the brain parenchyma, reducing intracranial plasma volume and pressure. Mannitol is a pharmacologically inert osmotic diuretic that inhibits reabsorption of water and sodium. It is given as a bolus intravenously in cases of cerebral edema. At a cellular level, mannitol does not cross the BBB but instead causes cell shrinkage from osmotic pressure and resultant stretching of transmembrane proteins, creating tiny holes in TJs (2). The use of mannitol for BBB disruption is controversial because of high rates of adverse effects including hypotension, seizure, and brain swelling. The major two effects of mannitol in the brain can be characterized as the rheological effect and osmotic effect. The rheological effect reduces blood viscosity and promotes plasma expansion and cerebral oxygen delivery (17). This leads to an auto regulation response of cerebral vasoconstriction and cerebral blood volume decrease. The second effect is based on the creation of an osmotic gradient across the BBB, leading to the movement of fluid from the brain into the intravascular space. When cells decrease in volume, the small holes that are generated at TJs permit access of water-soluble molecules (6).

2.2.4 In vitro Research

There are different types of *in vitro* BBB models and they each have advantages and disadvantages. The most physiologically accurate models involve primary human-

derived cells at very low passage numbers. Although no single model can perfectly

imitate the BBB, co-culture models that include cerebral microvascular endothelial cells,

pericytes, and astrocytes take into account the essential components of the NVU and

better recapitulate in vivo conditions (18). This and other advanced *in vitro* models that

use primary cells such as pluripotent stem cell-based models are time-consuming and

relatively expensive. Microfluidic models, often referred to as organ-on-a-chip models,

are currently being applied to validate delivery systems that transport drugs across the

BBB (19). Since microphysiological modeling is a new technique, the current technology

is relatively expensive and there are not any well-established models. The other available

options don't include the components of the NVU but are cheaper, more easily

reproduced, and easier to standardize. Epithelial cell monolayers and transwell

monocultures are less physiologically accurate but still express BBB characteristics that

can be monitored and tested. Overall, a clear need still exists to establish accessible assay

systems that test BBB disruption techniques and changes in permeability.

*2.3 Confocal Microscopy*

Confocal microscopy is extremely useful for optimal visualization of individual

cellular components. The application of different lasers and emission/excitation filters

makes it possible to analyze multicolor immunofluorescence in high resolution. Confocal

microscopes enable the creation of sharp images on single focus planes by blocking out

light from the background regions. Rather than illuminating the entire sample at once, the

lasers are directed onto a defined spot at a specific depth within the sample. A pinhole

inside the optical pathway effectively cuts off out of focus signals and allows only the

fluorescence from the illuminated spot to enter the detector. The microscope scans

specimens in a raster pattern (Figure 5) and creates images in a single optical plane (20).

Using the microscopy deconvolution software known as Z-stack, several images from

different optical planes can be stacked and help properly analyze 3D cellular structures.
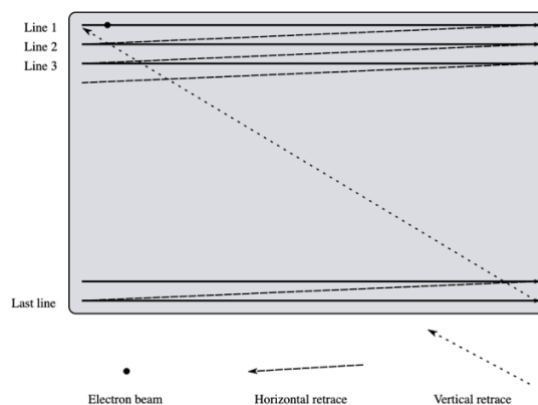


**Figure 5:** The confocal microscope raster scanning pattern of a specimen.

## 2.4 Electric Cell-substrate Impedance Sensing

Electric Cell-Substrate Impedance Sensing (ECIS) is a real-time accurate stress-

field monitoring technique that continuously measures the resistance, impedance, and

capacitance of a cellular monolayer in culture medium. It has the ability to reveal changes

in important behaviors such as cell death, monolayer opening, sonoporation, and cell

deplating. The software applies a mathematical model to data at multiple frequencies in

order to differentiate between junctional impedance, or the "tightness" of cell-to-cell

contact, substrate impedance, which is caused by cell-substrate interactions and depends

on the distance between the basal membrane and underlying matrix, as well as the

contribution of cell membrane capacitance. This model uses the smallest number of

elements to describe all features of the measured impedance spectrum to allow for

meaningful correlations (21).

**Figure 6:** ECIS 2W4x10E PC Electrode array. The 8 bean-shaped gold areas each contain 10 electrodes within their individual surface area (22).

2.4.1 Electric Circuit Components

Cells are grown in special culture chambers on top of opposing gold electrodes (Figure 6). A constant small alternating current is applied between the electrodes and the potential across is measured. When cells are brought into an electrical field, they begin to display properties of passive electronic components. As cells attach to the surface, they begin to restrict current flow by spreading over the electrodes. The insulating properties of cell membranes create an intrinsic resistance towards electrical current flow, which results in potential between electrodes. In an AC circuit the current and voltage differ in amplitude and phase. The complex impedance (Z) or magnitude of impedance is dependent on resistance (R) and reactance X(f):

$$|Z(f)| = \sqrt{R_C^2 + X(f)^2}$$

Measuring the complex impedance allows for the separation of overall impedance into ohmic resistance and reactance, which results from AC flow through capacitors causing the phase shift between voltage and current. Reactance is frequency dependent and dominated by the capacitive properties of the cell membrane:

$$X(f) = \frac{1}{2\pi f * C_C}$$

2.4.2 Equivalent Circuit

In order to interpret frequency dependent cellular properties from an impedance spectrum, a cell must act as a parallel connection of a resistor and a capacitor. The cellular electrical properties are represented by $R_c$ and $c_c$ in Figure 8. Resistance accounts for paracellular flow, which characterizes the integrity of the TJs. It is a direct measure of overall barrier quality, which is determined by the cells' ability to form cell-cell and cell-matrix interactions to block current flow. Lower frequencies force the current to travel under and between cells (Figure 7) and 4,000 Hz is the optimal measurement frequency for resistance as it neglects capacitive components.
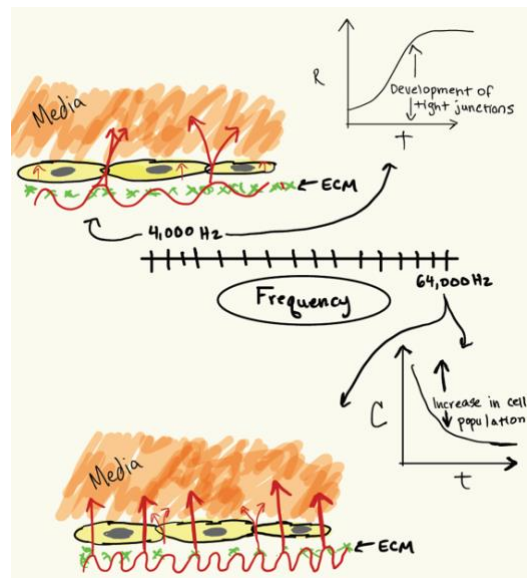


**Figure 7:** The effect of frequency on current pathways and electrical cell measurements.

Capacitance represents the separation of electric carriers at the bilayer of the cell membrane, which is the cause of cellular polarization. Adhesion, spreading, and proliferation can be quantified best from capacitance measurements at higher frequencies (64,000 Hz) because capacitance is directly proportional to electrode coverage and cell population (Figure 7). Therefore, as cells form a monolayer, capacitance decreases in a linear fashion as the percentage of open electrode area decreases.

All essential factors of the system are represented in the ECIS equivalent circuit (Figure 8), which includes the influences of the aforementioned cell components in parallel ($R_c$ and $c_c$), the resistance of the media ($R_m$), the resistance of cell-cell junctions ($R_{cleft}$) and the capacitance of the ECIS electrode.
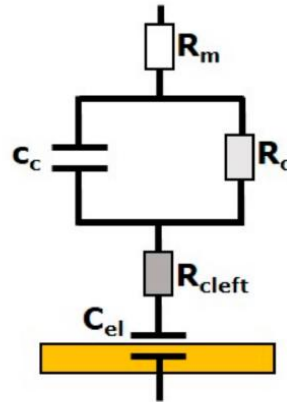


**Figure 8:** Equivalent circuit relating the cell layer contribution with the electrode and media influences (23).

## 2.4.3 Other Methods of Measuring TEER

ECIS possesses better measurement resolution and sensitivity compared to other methods that utilize transepithelial/endothelial electrical resistance (TEER). TEER readings are based on a voltage drop from a DC current that is applied to cells grown on permeable filters. TEER is often used to characterize paracellular transport mechanisms, and it outputs measurements in ohms*$cm^2$, which is the product of the well surface area and net resistance. The application of a direct current can cause adverse effects on both cells and electrodes and cannot measure frequency-dependent cell properties or differentiate between cell components. Additionally, TEER methods often require moving the measuring electrodes or removal from a regulated environment, which creates physiological disruption and error in resistance measurements (Figure 9).
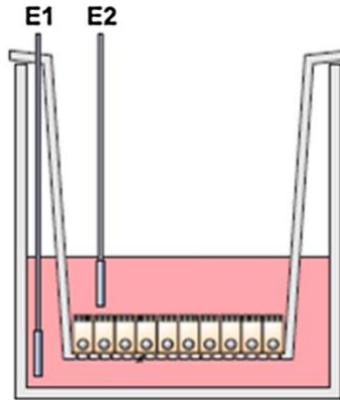
**Figure 9:** TEER Electrodes E1 and E2 are moved between wells creating physiological disruption (24).

Rather than taking measurements from cells grown on a porous membrane, ECIS cultures are grown on top of gold electrodes. The electrodes and cellular monolayer are in extremely close proximity to each other, which allows for high sensitivity measurements. However, the main caveat of the ECIS method is that there is no basolateral fluid compartment due to the adherence of cells to the electrode (24). This excludes ECIS as a relevant application for transport or transfer experiments.

# 3. MATERIALS AND METHODS

3.1 Cell Culture

This study focused on the behavior of TJs treated with mannitol. Human umbilical vein endothelial cells (HUVECs) form a layer of TJs and are commonly used for *in vitro* BBB models. HUVECs were used for the immunocytochemistry experiments because their architecture more accurately represents that of the BBB. However, difficulties in harvesting and purification of these cells can limit accessibility and reliability. Additionally, primary cells like HUVECs are used only at very low passage numbers to avoid down-regulation of BBB characteristics. The human hepatoma cell line (Hep3B) exhibits epithelial morphology and relies on tight junctions for barrier integrity as BBB cells do. Although they originate from the liver and do not exhibit all features of the human BBB, these epithelial cells quickly and easily grew cellular monolayers consisting of TJs and recapitulated the properties that were necessary for this experimental application. BBB endothelial cell connections are often referred to as 'epithelial-like' TJs because they are so tightly packed together. Therefore, Hep3B cells were used in ECIS experiments as an accessible alternative cell line to model TJ behavior for *in vitro* research.

HUVECs were cultured in sterile T-75 flasks and incubated at 37°C, 5% $CO_2$. Initially, each flask was coated with fibronectin ($1\mu g/cm^2$), a basement membrane protein that prevents cells from deplating and encourages them to stick to the flask. Flasks were immediately incubated for 2-12 hours. The fibronectin was removed after appropriate

incubation time and each flask received 8 ml of media, which consisted of Medium 200, LSGS and Gentamicin. 3000,000 – 500,000 (seeding density) HUVECs/cm$^2$ were seeded into each flask and left to incubate 2-3 days until media had to be replenished. Cells were visually monitored using a phase-contrast microscope. Hep3B cell culture followed a similar protocol to HUVEC cells but did not require fibronectin coating because of their tendency toward rapid growth. 500,000 Hep3b cells/cm$^2$ were seeded into each flask and required DMEM (Life Technology, Carlsbad CA) for nutrients.

3.1.2 Passaging Cells

Both types of cells were passaged every 7 days. Media was removed and cells were washed with phosphate-buffered saline (PBS), which removes any residual media. Next, 2 ml of Trypsin-EDTA (0.25%, (Life Technology, Carlsbad CA)) were added and flasks were incubated for 5 minutes. Following trypsinization, which removed adherent cells from the bottom of the flask, 3 ml of media were added to inactivate the trypsin. After this, 20 μl of solution were removed for cell counting and added to 480μl of PBS (pH 7.4, ThermoFisher Scientific, Waltham, MA, USA) in a microcentrifuge tube. After being vortexed for a 2-3 seconds, the tube was put in the flow cytometer, which then determined the number of cells in the tube. The remaining solution was centrifuged for 5 minutes at 1000 RPM and 25°C and caused the cells to separate from the solution and collect at the bottom of the tube. After removing the media and trypsin from the centrifuge tube without disturbing the cell pellet, an appropriate volume of media was added to achieve a simple cell number to volume ratio such as 1 million cells/ml. Finally, the cell solution was distributed evenly between new flasks and media was added accordingly so each flask resulted in the same volume of media/cell solution.

3.2 Staining

As HUVECs proliferated and reached close to 3,000,000, a 24-well plate was prepared for culture by coating with fibronectin ($1\mu g/cm^2$) and leaving the plate to incubate for 2 hours. After aspirating fibronectin from each well, 0.7 ml of media (Medium 200 and LSGS) were added and HUVECs were seeded at a density of 120,000 cells/well and left to incubate overnight. Mannitol solutions were made by heating deionized water and mannitol powder to 37 °C and mixing at 200 RPM for 10 minutes. After incubation and media removal, three solutions (0 M, 0.5 M, 1.0 M) of mannitol were added to designated wells. Mannitol solutions were aspirated after sitting for 20 minutes in room temperature. In order to fix the cells as the mannitol took affect but before the recovery began, cells were rinsed in cold PBS immediately following mannitol aspiration and coated with 500 μl/well of -20°C methanol (25). The well-plate was left to fix and permeabilize for 15 minutes in the fridge on top of a bed of ice. After cautiously aspirating the methanol, 350 μl of PBS were added to each well and again were left to sit in room temperature for 5 minutes. This PBS wash was repeated three times to ensure that the methanol was completely washed away. Lastly, 350 μl of protein block, which consisted of PBS, 5% Normal Goat serum (ThermoFisher Scientific, Waltham, MA) and 0.3% Triton X-100, were added to each well and left to sit with the lid on in room temperature for an hour.

A staining validation experiment was conducted prior to this experiment in order to determine the following primary and secondary antibody concentrations. The primary antibody used in this experiment was rabbit anti-VE cadherin, an intracellular junction marker (ThermoFisher Scientific, Waltham, MA). Following the protein block, cells were treated with a primary antibody solution that consisted of 0.1 μg/ml rabbit anti-VE cadherin

in a buffer solution of PBS, 1% Bovine Serum Albumin (BSA), and 0.3% Triton-X. After

overnight incubation, the secondary antibody solution of goat anti-rabbit IgG H&L (HRP,

ThermoFisher Scientific, Waltham, MA) with a concentration ratio of 1:1000 in the same

buffer was added to each well. After aspirating, all wells were washed with DPBS and left to

sit for 5 minutes. Next, 350 µl/well of 1µg/ml Hoechst in DPBS were added and covered with

foil in room temperature for 7 minutes. Finally, each well was emptied and washed twice

with DPBS for five minutes. After removing the DPBS, 350 µl of PBS were added to prepare

for imaging.

## 3.3 Imaging

A 10x objective was used to image each well and z-stacks were taken at a pixel

size of 2048. The pinhole was set to 1.9 Angstroms and the pixel dwell was at 5 µm. In

order to capture accurate images, an optical zoom of 6x was used to achieve a total 60x

magnification. Z-stack processing allowed for multiple images at different focal points to

be compiled, creating an image with a greater field depth. All confocal images were

processed and scaled identically to reduce any chance of visual variability.

## 3.4 ECIS Experiment

Hep3B cells were used to conduct ECIS experiments due to accessibility and

reproducibility concerns. Once cells reached 80% confluence, 1,500,000 cells were

seeded in each well of the ECIS chip. First, 1 ml of cystine (Applied BioPhysics Inc,

Troy, NY), a binding agent for the metal electrodes that cleans and modifies the electrode

surface, was added to each well for 10 minutes. Cystine is an integral part of the chip

preparation because it reduces variability by providing a high and reproducible electrode capacitance. After rinsing twice with deionized water, 300 ml of fibronectin were added to each well and incubated for 2 hours. The wells were covered with Tegaderm, which is gas-permeable, allowing for $CO_2$ transfer, but not liquid permeable so the media cannot evaporate. After removing the fibronectin, the wells were rinsed with deionized water one more time before adding cells.

Once cells are seeded and left to grow overnight with 2 ml of media in each well, the chip was plugged into the ECIS machine. Mannitol was dissolved in media rather than deionized water for ECIS experiments in order to prevent additional factors that could potentially affect resistance measurements. For the initial experiment, after an hour of the software collecting baseline data, 2 ml of 0.5 M mannitol solution was added to the well closest to the connection to the machine.1.0 M mannitol solution was added to the farther well (Figure 10). The solutions were mixed carefully using a 200 μl pipette and the acute stimulus time point was marked. Data collection resumed for another hour and then paused again for mannitol solution removal. 2 ml of media were added to each well and ECIS data was collected overnight.
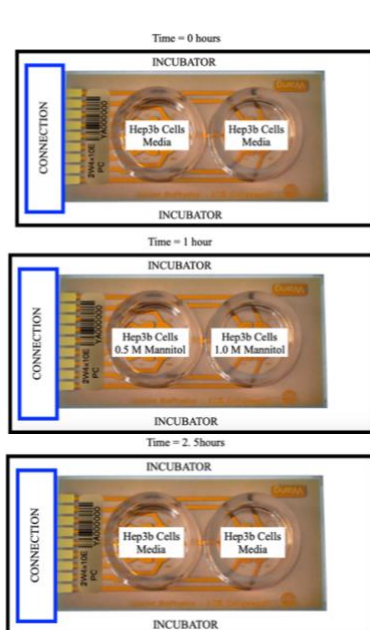
**Figure 10:** Experimental Electrode Array at time = 0, 1, 2.5 hours.

The second experiment focused on both mannitol concentration and duration of exposure. Two ECIS chips were used for data collection, resulting in four separate experimental wells. After an hour of data collection, 1.0 M mannitol solution was administered to one well and left for 2 minutes. At the end of 2 minutes, the mannitol solution was removed, and the well was rinsed once with media. Then, the other well was treated with 1.0 M mannitol for 10 minutes. After removing and rinsing, both wells received new media and were monitored until resistance data plateaued. This procedure was repeated on a new chip with 1.0 M mannitol treatment times of 15 and 20 minutes.

An additional imaging experiment was conducted using a 24-well plate seeded with Hep3B cells. After 24 hours of incubation, each well was imaged, and old media was removed. Wells were treated with either 1.0 M or 0.5 M mannitol concentration at different exposure durations. Immediately following mannitol removal, the cells were imaged using a phase contrast microscope in order to visualize the immediate effects that were observed in ECIS monitoring.

# 4. RESULTS

4.1 Confocal Microscopy Imaging Analysis

Post-imaging analysis of stained HUVEC monolayers determined that the appearance of TJs were significantly different after exposure to various concentrations of mannitol (Figure 11) compared to the control, which was imaged after one wash of deionized water. The cadherin-targeted fluorescent dye made it possible to analyze high-quality images of the membranes and identify the spaces between each individual cell. There were notable differences in cell morphology. The control case failed to exhibit a confluent monolayer and there was not a normal amount of cell-cell contact. However, cells treated with 0.5 M mannitol appeared to be confluent and no junctional spaces could be distinguished. The green dye appeared to stain the edges of the membrane in these images and the nucleus was easily distinguished. The 1.0 M mannitol-treated cell layer appeared to have spaces between individual cells. The green stain was significantly less apparent at the edges of the cells in the 1.0 M mannitol, but the entire cell body appeared to be stained. The nuclei stained with Hoechst were still easily identifiable. The 1.25 M and 1.50 M images looked as if the cells had died before they were fixed. There were notable differences in the degree of fluorescence exhibited and the cell bodies looked to be shriveled while the TJs were difficult to make out. This staining experiment provided guidance when deciding on what concentrations to use in ECIS experiments.
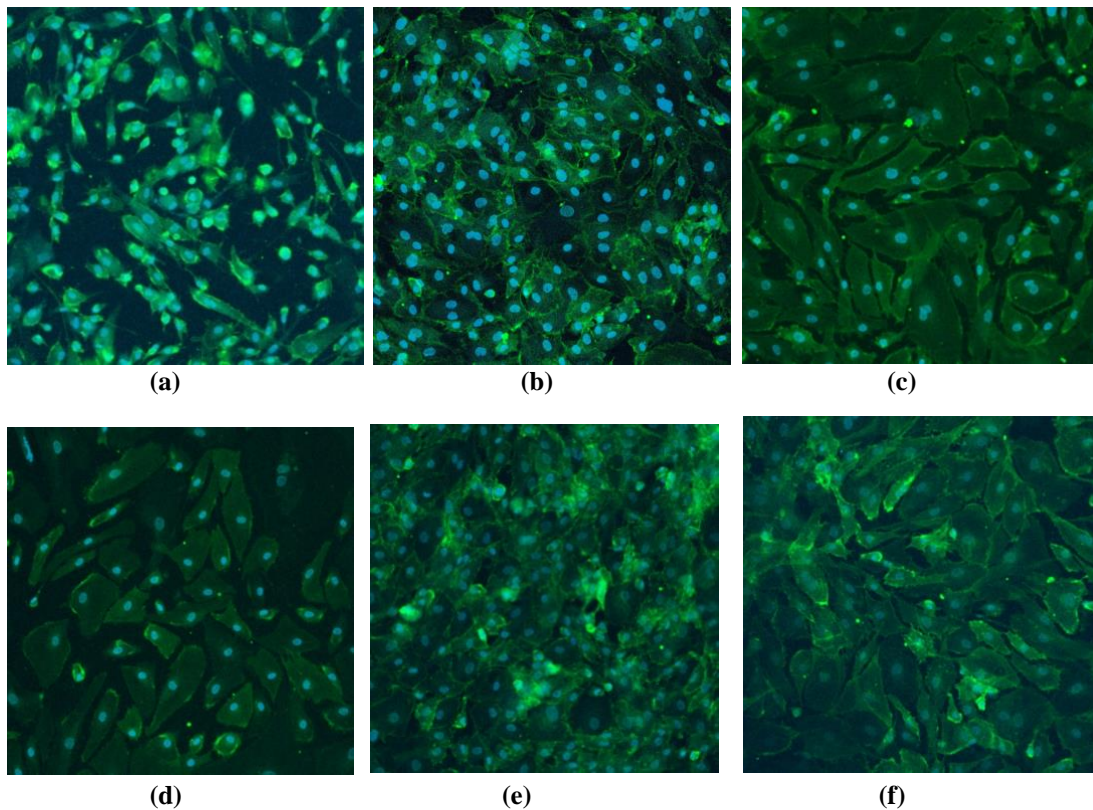
**Figure 11:** Confocal images of stained HUVEC cells after 20-minute variable exposure to mannitol solutions of **(a)** 0 M Mannitol (control), **(b)** 0.5 M Mannitol, **(c)** 0.75 M Mannitol, **(d)** 1.0 M Mannitol, **(e)** 1.25 M Mannitol, **(f)** 1.50 M Mannitol

## 4.2 Phase Contrast Microscopy Imaging Analysis

Phase contrast images of Hep3B cells immediately prior to and after mannitol treatment were not as revealing as the fluorescent confocal images. There were some noticeable changes in barrier integrity but the visual data from this experiment was inconclusive because of variability in exposure and focus settings. The images in Figure 12 are before and after cases of the same experiment (20-minute 1.0 M Mannitol exposure) repeated twice.
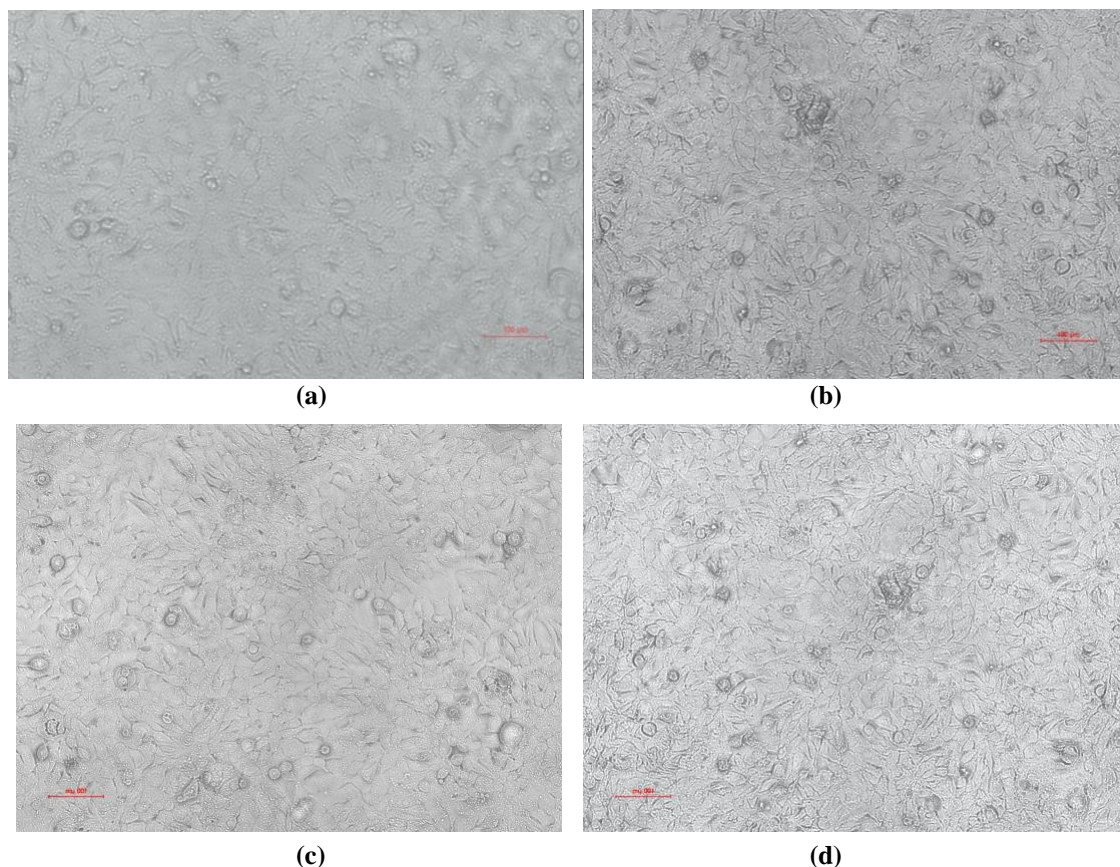
**Figure 12:** Phase contrast images of Hep3B cells **(a)** Before 1.0 M mannitol exposure, **(b)** Immediately following 20 minutes of 1.0 M Mannitol exposure, **(c)** Second run of experiment before 1.0 M mannitol exposure, **(d)** Immediately following 20 minutes of 1.0 M Mannitol exposure

## 4.3 Electrode Array Imaging Analysis

Initial images of the electrodes showed a confluent monolayer of cells covering the bean area and all electrodes. Only portions of the bean were imaged but all were checked for full confluency before plugging into ECIS machine for data collection (Figure 13). The post-imaging analysis showed significant damage to the 1.0 M mannitol-treated monolayer (Figure 14). Little to no cells were covering the electrodes and the monolayer appeared completely destroyed. The 0.5 M mannitol monolayer did appear to have sustained some damage but still had visible cells attached to electrodes (Figure 13).

Imaging the electrode array before and after the experiment served as a verification for the results collected during impedance sensing.
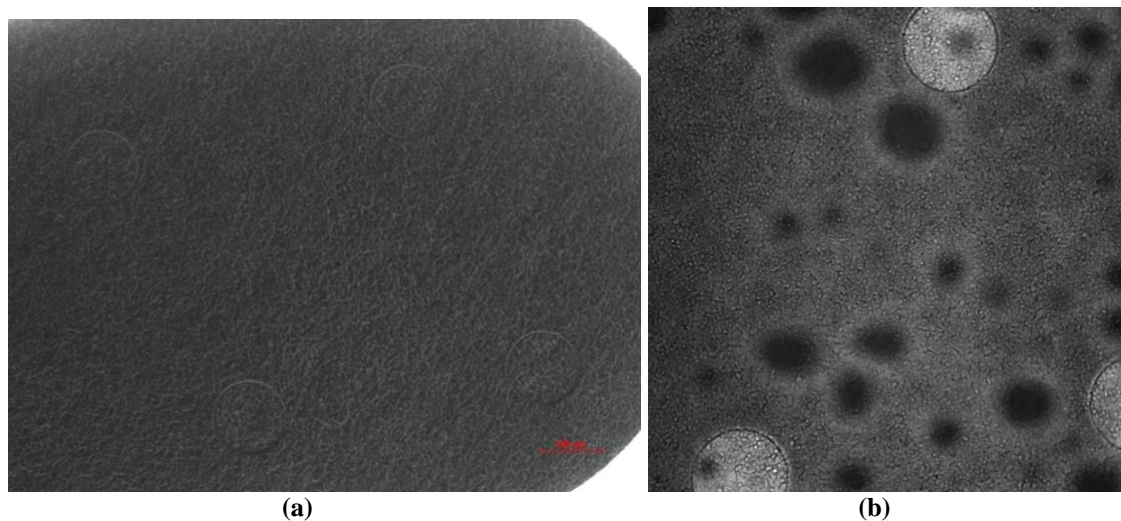


**Figure 13:** Phase contrast images of Hep3b cellular monolayer on ECIS chip **(a)** Bean 5 before 0.5 M mannitol 90-minute treatment, **(b)** Bean 5 after treatment
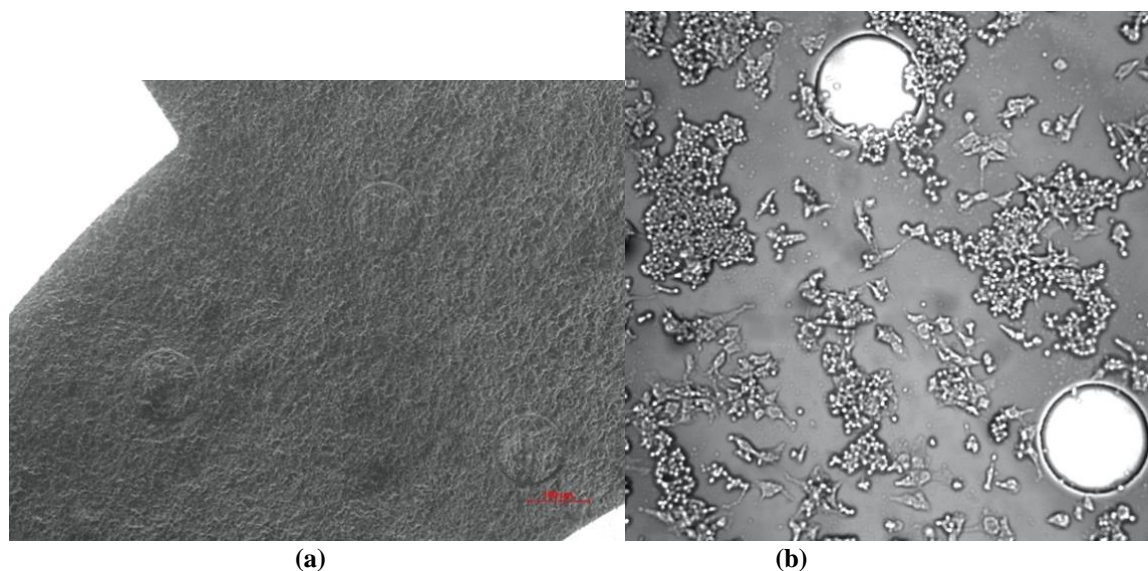


**Figure 14:** Confocal bright field images of Hep3B cellular monolayer on ECIS chip post mannitol treatment **(a)** Bean 5 after 0.5 M Mannitol, **(b)** Bean 7 after 1.0 M Mannitol

The individual imaging of each bean before and after hyperosmotic exposure corresponded to the electrical changes in capacitance and resistance. For example, the cell death or deplating that was visually apparent from the 90-minute exposure to 1.0 M mannitol was represented by a sharp increase in capacitance (Figure 15). These images confirmed the relationship between capacitance changes and likely captured TJs responding to mannitol through changes in resistance and immunocytochemical results.

## 4.4 ECIS Analyses

ECIS provided useful insights regarding the cellular mechanisms of mannitol-induced hyperosmotic shock. Changes in cell behavior were successfully monitored and validated through imaging techniques. The TEER of the intercellular cleft was measured at 4,000 Hz and outputted two different reactions to 1.0 and 0.5 M mannitol solutions.
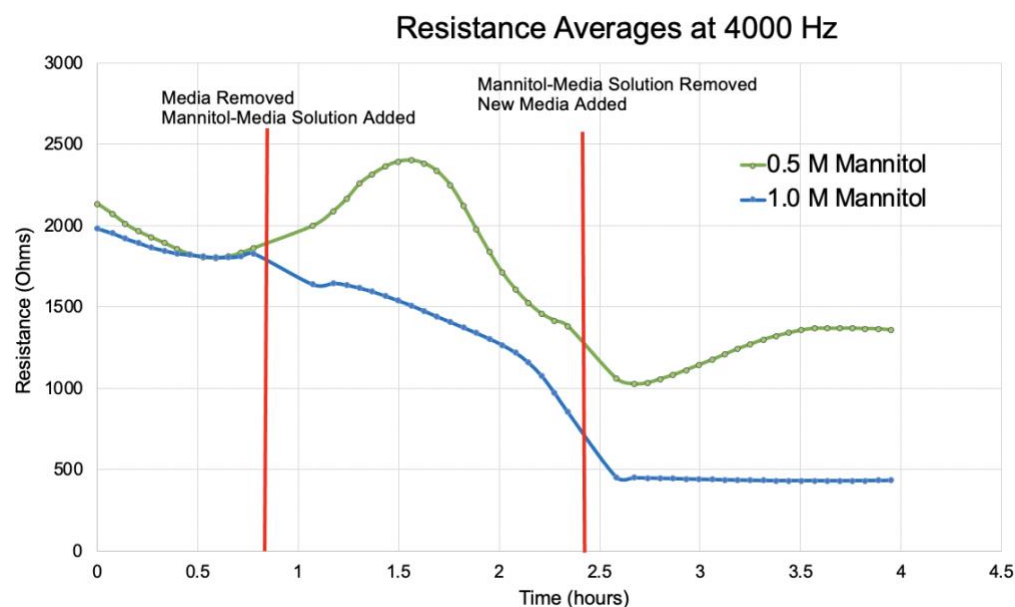


**Figure 15:** The average resistance changes at 4,000 Hertz for 1.0 M Mannitol treatment of two different concentrations. The red lines indicate when the ECIS software was paused, and the incubator opened to put mannitol or culture medium in each well.

Both wells stabilized at an average baseline value of 1765 Ohms. As mannitol was added, ECIS software quantified the electrical changes of the cellular monolayer in real-time. There is an initial spike in electrical values for the 0.5 M mannitol-treated cells followed by a major decrease in impedance and resistance. Mannitol was administered at time 0.9 hours, corresponding with the change in resistance. The 1.0 M resistance values stayed below 500 Ohms after mannitol removal and post-experiment pictures revealed significant deplating and damage to the original monolayer.

Linear decreases in resistance at lower frequencies such as 4,000 Hz represent the spreading out of tight junctions that is a result of osmotic shrinkage. Therefore, the 0.5 M monolayer most likely experienced changes in barrier integrity from 1.5 to 2 hours. The return to baseline resistance values represents barrier recovery. The 1.0 M mannitol-treated monolayer resistance started to decrease immediately and eventually stabilized under 500 ohms. Figure 16 shows that most cells were killed in the 1.0 M mannitol well and only some were killed in the 0.5 M mannitol because of the minor increase in capacitance relative to 1.0 M changes.
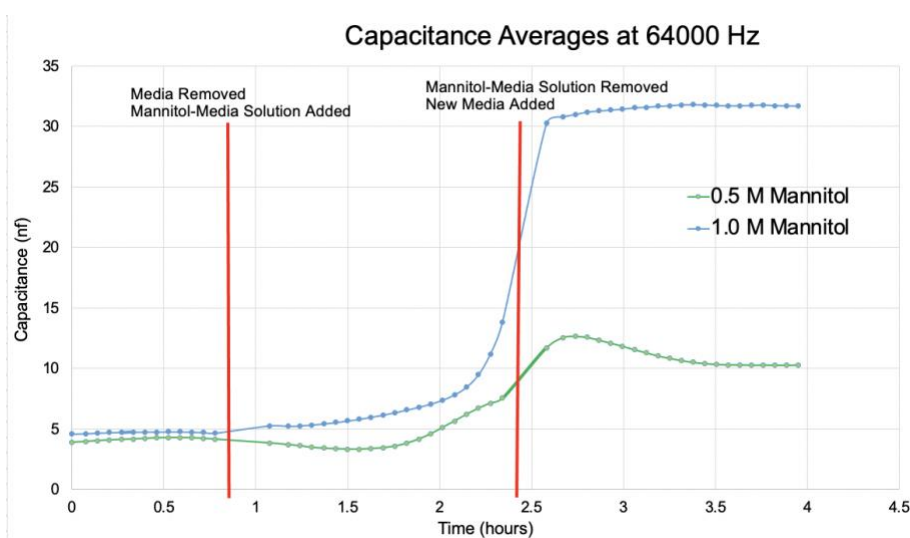


**Figure 16:** The 1.0 M mannitol-treated monolayer capacitance shows a rapid increase, which represents the deplating of cells or cell death on top of the electrodes.

The results of this initial concentration experiment prompted the question of exposure time and whether that might have a stronger influence on how cells react. 1.0 M mannitol was used in the following experiments because it is closer in range to clinically relevant concentrations that are usually somewhere near 1.4 M. For the next experiment, two beans were not covered with cells (Figure 17), so the data collected from those wells were not included in calculated experimental averages. Figure 18 shows the resistance over time after one well was treated with 2 minutes of 1.0 M mannitol, which is the portion of the red curves starting at the orange line and ending at the blue. The green lines represent the 10-minute exposure, which started at the blue line and ended at the green vertical line. The horizontal blue line represents bean 1 and 2, which showed a steady average of 500 Ohms throughout the entirety of the experiment.
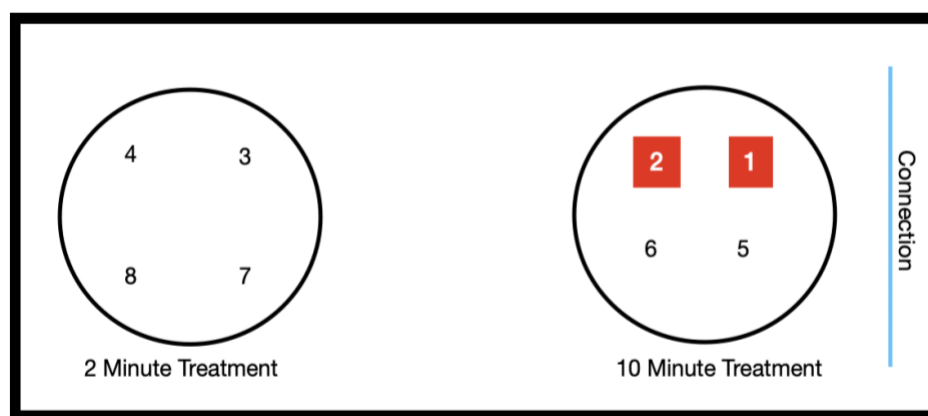


**Figure 17:** The experimental set-up. The red numbers represent the beans that had no cells on them and stayed around 500 Ohms.
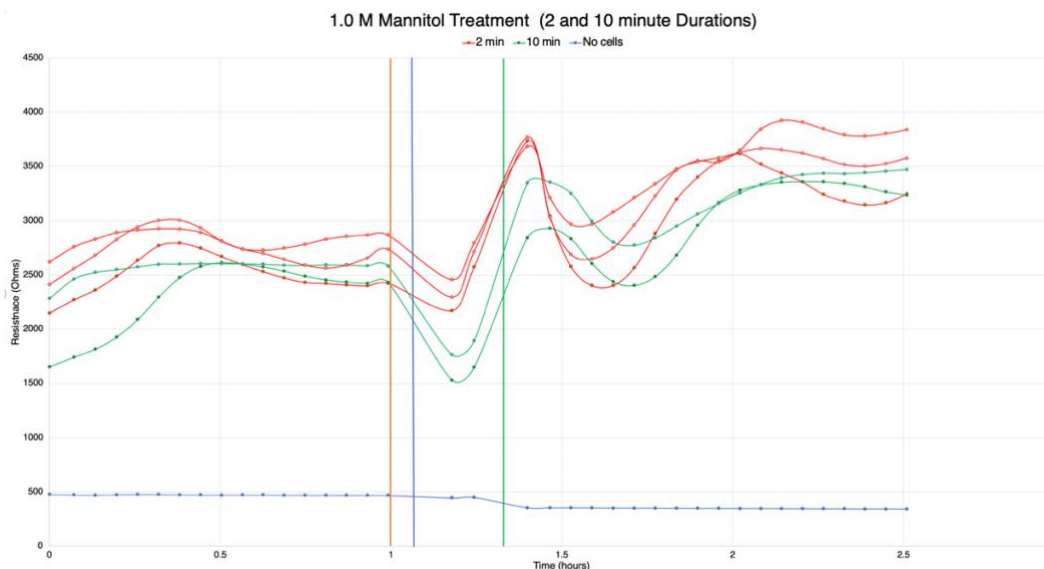
**Figure 18:** The 2-minute 1.0 M mannitol treatment (red lines) showed a decrease in resistance of 699 Ohms. The 10-minute 1.0 M mannitol treatment (green lines) showed a decrease of 877 Ohms.

The following experiment was conducted using 0.5 M Mannitol treatments as 15-and 30-minute exposure durations (Figure 19). The 15-minute exposure began at the vertical yellow line and ended at the blue vertical line. The changes in resistance showed an immediate decrease in resistance for around 10 minutes and the start of recovery before the mannitol solution was removed. The 30-minute resistance changes showed a larger decrease in resistance but also seemed to start barrier recovery before the exposure time ended. The 0.5 M mannitol results did not follow the same pattern as 1.0 M mannitol treated cells did, which means that the cells reacted differently to the concentrations.
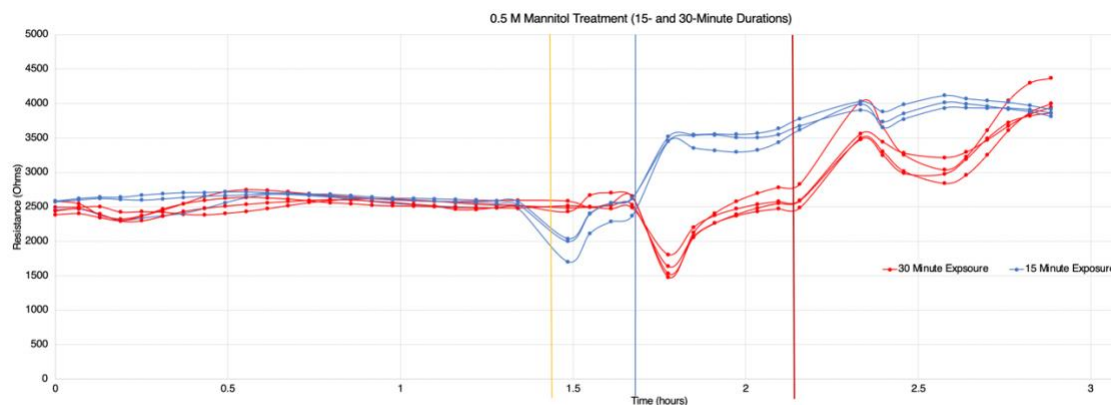
**Figure 18:** The changes in resistance for 0.5 M Mannitol treatment at 15- and 30-minute exposure times.

The final experiment was conducted using 1.0 M mannitol in order to further test the relationship between a clinically relevant concentration of mannitol and exposure time (Figure 19).

1.0 M Mannitol Treatment (15- and 20-minute Durations)
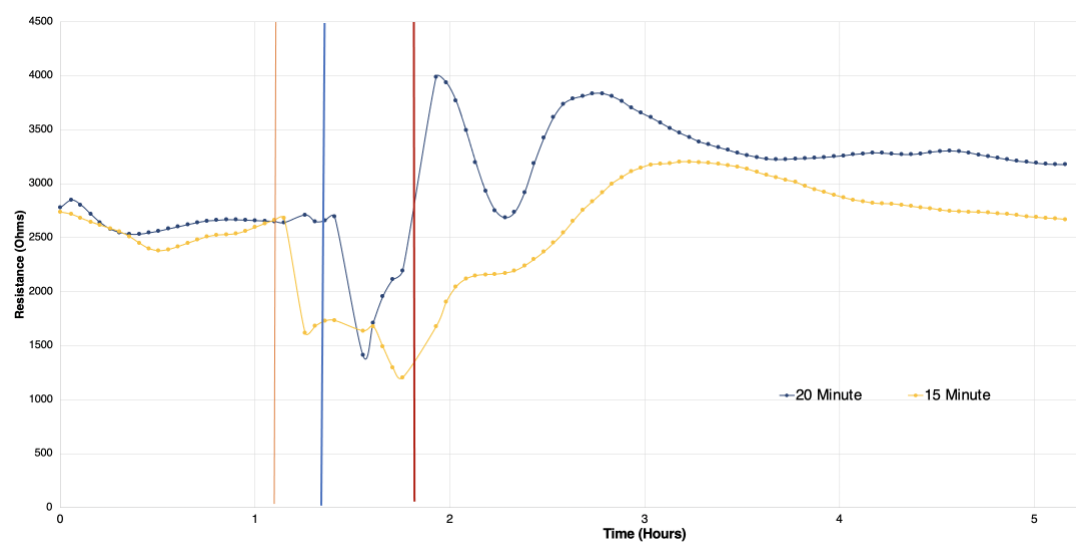


**Figure 19:** The changes in resistance for 1.0 M Mannitol treatment at 15- and 20-minute exposure times.

The 15-minute exposure time resulted in the largest drop in resistance and appeared to recover and reach its baseline value after two hours. There appeared to be an

initial drop in resistance that was followed by another drop in resistance, and then progressive recovery. The 20-minute exposure time showed an expected drop in resistance and recovery time. It is interesting to note that although the drop in resistance was larger for the 15-minute well, the recovery for the 20 minutes well was much faster and much more significant. However, both cases appeared to make a full recovery and verify the transient nature of mannitol's effect.

.

# 5. DISCUSSION

Results showed transient opening of TJs in both cancerous cells and HUVECs –
providing a more complete understanding of BBB mechanisms and CNS drug delivery
methods. The 0.5 M mannitol image showed separation between the stained nucleus and
membrane but did not present any spaces between individual cells. The 1.0 M mannitol
treatment showed nucleus and membrane distinction as well as individual cell shrinkage
and junction separation. Confocal images acted as a guided for the concentration
selection for ECIS experiments. The staining experiment elucidated functional and
molecular hyperosmotic changes of TJs in BBB.

Initially, the ECIS experiment was conducted using mannitol dissolved in deionized
water, which was what was used for the stained HUVEC/mannitol experiment. Although
the resulting images taken on the confocal microscope proved that mannitol-treated cells
at specific concentrations do shrink and open up TJs, the deionized water-mannitol
solution majorly skewed ECIS data. The addition of deionized water had a significant
effect on the conductance of the media and subsequent resistance measurements. In order
to avoid that source of variability, mannitol dissolved in media was used for all reported
experiments. Therefore, the only difference between the baseline value measurements
and the chemically treated measurements was the addition of a hypertonic cellular
environment. Using the same concentration of mannitol, the exposure time made a
significant difference in the maximum drop in resistance (Figure 20). The largest changes

were seen in the shorter time durations (2-20 minutes) with the greatest change measured

at a 15-minute exposure time with a value of 1455 Ohms.
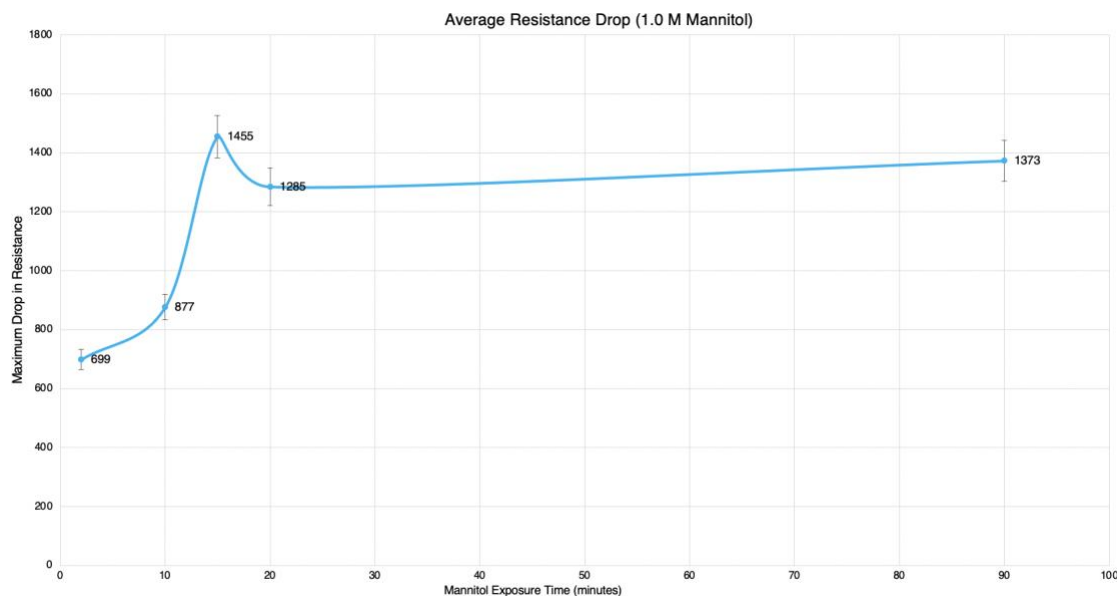


**Figure 20:** The maximum drop in resistance based on 1.0 M mannitol exposure time. All cases made over 100% recovery beside the 90-minute exposure.

Future work on this project could include the addition of live-cell monitoring of

hyperosmotic mechanisms using an advanced live-cell imaging technique such as

Incucyte monitoring. Therefore, it would be possible to conduct the analysis of

fluorescently labeled images of live cells rather than cells that were killed and fixed

during mannitol treatment. This would enable the visualization of barrier recovery and

identification of real-time changes in morphology and behavior. Additionally, it would be

interesting to analyze the differences of Hep3B and HUVEC cellular response to

hyperosmotic shock. This could reveal insights on how cancerous cells would react when

exposed to mannitol and present differences between epithelial and endothelial electro-

physiological properties and barrier integrity. A co-culture that includes essential

components of the NVU such as pericytes and astrocytes could be applied to the

procedures in this research, which would allow for the testing of a more physiologically accurate BBB model that embodies multiple regulatory components of barrier permeability. Future investigation into cellular reactions to low concentrations of mannitol such as 0.5 M should be continued because it would increase the understanding of how concentration affects cell behavior and whether or not smaller concentrations exhibit delayed effects. Overall, the novelty of this experiment is the testing of hyperosmotic mechanisms in a controlled environment. Other TEER methods have been used to measure mannitol's effects but have often found data to be unreliable because of external movement of electrodes and physical disruption of the barrier during measurements.

The changes in cellular behavior are heavily dependent on mannitol concentration and duration of exposure. The results of this project point toward mannitol as an effective agent for barrier disruption as long as precise clinical parameters are established. The procedures applied in this work have the potential to improve *in vitro* permeability testing and help with the determination of parameters and conditions that produce an optimum duration of disruption without resultant neurotoxicity.

# 6. CONCLUSION

This study analyzed the chemical disruption of the tight and adherens junctional complex and quantified changes in cellular behavior using impedance data and microscopy techniques. Results established a strong foundation for testing various stimuli in ECIS and accurately monitoring monolayer permeability and intercellular changes. The procedure for successful visualization of hyperosmotic cellular reaction was developed and verified. The combination of electrical and visual data revealed valuable insights into tight junction behavior after hyperosmotic shock.

# <u>REFERENCES</u>

1.  Pardridge, W. M. (2005). The blood-brain barrier: Bottleneck in brain drug development. *Neurotherapeutics*, *2*(1), 3–14. https://doi.org/10.1007/bf03206638

2.  Linville, R. M., DeStefano, J. G., Sklar, M. B., Chu, C., Walczak, P., & Searson, P. C. (2019). Modeling hyperosmotic blood–brain barrier opening within human tissue-engineered in vitro brain microvessels. *Journal of Cerebral Blood Flow & Metabolism*, *40*(7), 1517–1532. https://doi.org/10.1177/0271678x19867980

3.  Feigin, V. L., Nichols, E., Alam, T., Bannick, M. S., Beghi, E., Blake, N., … Vos, T. (2019). Global, regional, and national burden of neurological disorders, 1990–2016: a systematic analysis for the Global Burden of Disease Study 2016. *The Lancet Neurology*, *18*(5), 459–480. https://doi.org/10.1016/s1474-4422(18)30499-x

4.  Peters, N. A., Farrell, L. B., & Smith, J. P. (2018, January 19). Hyperosmolar Therapy for the Treatment of Cerebral Edema. *US Pharmacist*. https://www.uspharmacist.com/article/hyperosmolar-therapy-for-the-treatment-of-cerebral-edema.

5.  Ikeda, M., Bhattacharjee, A. K., Kondoh, T., Nagashima, T., & Tamaki, N. (2002). Synergistic Effect of Cold Mannitol and Na+/Ca2+ Exchange Blocker on Blood–Brain Barrier Opening. *Biochemical and Biophysical Research Communications*, *291*(3), 669–674. https://doi.org/10.1006/bbrc.2002.6495

6.  Tajes, M., Ramos-Fernández, E., Weng-Jiang, X., Bosch-Morató, M., Guivernau, B., Eraso-Pichot, A., … Muñoz, F. J. (2014). The blood-brain barrier: Structure, function and therapeutic approaches to cross it. *Molecular Membrane Biology*, *31*(5), 152–167. https://doi.org/10.3109/09687688.2014.937468

7.  Lu, W. (2012). Adsorptive-Mediated Brain Delivery Systems. *Current Pharmaceutical Biotechnology*, *13*(12), 2340–2348. https://doi.org/10.2174/138920112803341851

8.  Bell, A. H., Miller, S. L., Castillo-Melendez, M., & Malhotra, A. (2020). The Neurovascular Unit: Effects of Brain Insults During the Perinatal Period. *Frontiers in Neuroscience*, *13*. https://doi.org/10.3389/fnins.2019.01452

9.  Kadry, H., Noorani, B., & Cucullo, L. (2020). A blood–brain barrier overview on structure, function, impairment, and biomarkers of integrity. *Fluids and Barriers of the CNS*, *17*(1). https://doi.org/10.1186/s12987-020-00230-3

10. McConnell, H. L., Kersch, C. N., Woltjer, R. L., & Neuwelt, E. A. (2017). The Translational Significance of the Neurovascular Unit. *Journal of Biological Chemistry*, *292*(3), 762–770. https://doi.org/10.1074/jbc.r116.760215

11. Daneman, R., & Prat, A. (2015). The Blood–Brain Barrier. *Cold Spring Harbor Perspectives in Biology*, *7*(1). https://doi.org/10.1101/cshperspect.a020412

12. Huber, J. D., Egleton, R. D., & Davis, T. P. (2001). Molecular physiology and pathophysiology of tight junctions in the blood–brain barrier. *Trends in Neurosciences*, *24*(12), 719–725. https://doi.org/10.1016/s0166-2236(00)02004-x

13. Campbell, H. K., Maiers, J. L., & DeMali, K. A. (2017). Interplay between tight junctions & adherens junctions. *Experimental Cell Research*, *358*(1), 39–44. https://doi.org/10.1016/j.yexcr.2017.03.061

14. Burgess, A., Shah, K., Hough, O., & Hynynen, K. (2015). Focused ultrasound-mediated drug delivery through the blood–brain barrier. *Expert Review of Neurotherapeutics*, *15*(5), 477–491. https://doi.org/10.1586/14737175.2015.1028369

15. Bellettato, C. M., & Scarpa, M. (2018). Possible strategies to cross the blood–brain barrier. *Italian Journal of Pediatrics*, *44*(S2). https://doi.org/10.1186/s13052-018-0563-0

16. Kapila, S. (2005, March). *Mannitol-ICU*. Society of Trauma Nurses. https://www.traumanurses.org/_resources/resource_library/clinical_practices_and_guidelines/mannitol_icu.pdf?phpMyAdmin=YUKhXpm3NuRfJ3YccE22H8dYHvf.

17. Davis, M., & Lucatorto, M. (1994). Mannitol Revisited. *Journal of Neuroscience Nursing*, *26*(3), 170–174. https://doi.org/10.1097/01376517-199406000-00012

18. Bagchi, S., Chhibber, T., Lahooti, B., Verma, A., Borse, V., & Jayant, R. D. (2019). In-vitro blood-brain barrier models for drug screening and permeation studies: an overview. *Drug Design, Development and Therapy*, *Volume 13*, 3591–3605.

19. Park, T.-E., Mustafaoglu, N., Herland, A., Hasselkus, R., Mannix, R., FitzGerald, E. A., … Ingber, D. E. (2019). Hypoxia-enhanced Blood-Brain Barrier Chip recapitulates human barrier function, drug penetration, and antibody shuttling properties. *Nature Communications*. https://doi.org/10.1101/482463

20. *Microscopy Techniques: Confocal Microscopy*. ibidi. https://ibidi.com/content/216-confocal-microscopy.

21. Szulcek, R., Bogaard, H. J., & van Nieuw Amerongen, G. P. (2014). Electric Cell-substrate Impedance Sensing for the Quantification of Endothelial Proliferation, Barrier Function, and Motility. *Journal of Visualized Experiments*, (85). https://doi.org/10.3791/51300

22. *2W4x10E PC (Specialty PC)*. Applied BioPhysics Inc. (n.d.). https://applied-biophysics-inc.myshopify.com/collections/specialty-arrays/products/2w4x10e-pc-specialty-array.

23. Robilliard, L., Kho, D., Johnson, R., Anchan, A., O'Carroll, S., & Graham, E. (2018). The Importance of Multifrequency Impedance Sensing of Endothelial Barrier Formation Using ECIS Technology for the Generation of a Strong and Durable Paracellular Barrier. *Biosensors*, *8*(3), 64. https://doi.org/10.3390/bios8030064

24. Benson, K., Cramer, S., & Galla, H.-J. (2013). Impedance-based cell monitoring: barrier properties and beyond. *Fluids and Barriers of the CNS*, *10*(1), 5. https://doi.org/10.1186/2045-8118-10-5

25. Jacob, A.-M., & Gaver, D. P. (2012). Atelectrauma disrupts pulmonary epithelial barrier integrity and alters the distribution of tight junction proteins ZO-1 and claudin 4. *Journal of Applied Physiology*, *113*(9), 1377–1387. https://doi.org/10.1152/japplphysiol.01432.2011

# <u>BIOGRAPHY</u>

Natalie Schwartz is the daughter of Kenneth and Colette Schwartz and sister of Carly Schwartz. She attended Springside Chestnut Hill Academy in Philadelphia from Kindergarten through high school. She has spent her last five years earning her Bachelor's and Master's in Biomedical Engineering from Tulane University. After graduation, she is moving to Chicago to continue working on the neurology and psychiatry team for Tempus, a biotechnology company focused on data-driven precision medicine.